

# Form finding of stress adapted folding as a lightweight structure under different load cases

Juan MUSTO\*, Max LYON, Martin TRAUTZ, Leif KOBELT

RWTH Aachen University  
Schinkelstr. 1, 52062 Aachen, Germany  
musto@trako.arch.rwth-aachen.de

## Abstract

In steel construction, the use of folds is limited to longitudinal folds (e.g. trapezoidal sheets). The efficiency of creases can be increased by aligning the folding pattern to the principal stresses or to their directions. This paper presents a form-finding approach to use the material as homogeneously as possible. In addition to the purely geometric alignment according to the stress directions, it also allows the stress intensity to be taken into account during form-finding. A trajectory mesh of the principle stresses is generated on the basis of which the structure is derived. The relationships between the stress lines' distance, progression and stress intensity are discussed and implemented in the approaches of form-finding. Building on this, this paper additionally deals with the question of which load case is the most effective basis for designing the crease pattern when several load cases can act simultaneously.

**Keywords:** lightweight-construction; folding; principle stress lines; Mixed-Integer Quadrangulation

## 1 Introduction

Besides membrane and shell structures, folding structures are among the most efficient design principles that can achieve relatively high load-bearing capacities with minimal material input. In lightweight construction, this principle is primarily used with thin-walled, flat, semi-finished products. In addition to conventional axial longitudinal foldings in the form of trapezoidal or corrugated sheets, space fold structures and fold-core-plates (also known as sandwich panels) are examples of this design principle, consisting of a folding core and a top/bottom cover layer [1]. In addition to the fact that the mechanical cross-section values are significantly increased by folding a flat material, the favourable static load-bearing behaviour of folding constructions is reinforced by the following phenomenon: If one considers the stress pattern of a folding construction, it is notable that the stresses are predominantly “bundled” over the stabilizing folding edges.

In this paper, we make use of this load bearing behaviour to increase the efficiency a folding structure by aligning the folding pattern to the principal stress directions.

## 2 Related Work

In steel construction, almost all form-finding processes are parametric structural optimization oriented (PSO). In PSO individual design parameters (e.g. height, sheet thickness and distances) are calculated iteratively with the help of genetic algorithms in order minimize the amount of

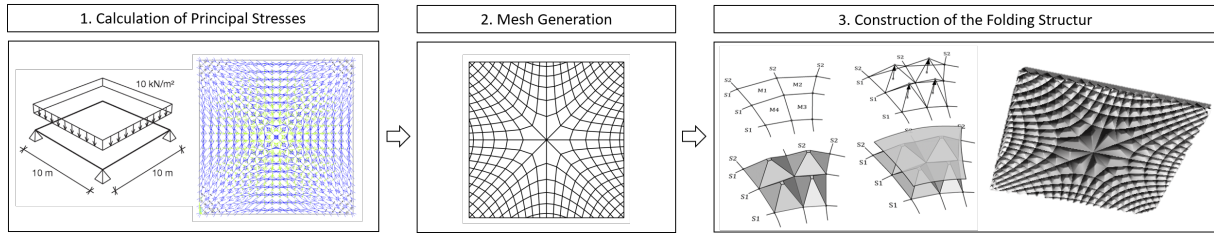


Figure 1: Process to construct the stress adapted fold structure.

material on the Object, rather than a geometric alignment of the load-bearing elements according to previously calculated “load paths”.

In the CIAB Pavilion Beijing [2] the principle of load paths was realized with a bar structure. The bars, which form the geometry, are aligned with the principle stress direction at the same time. Researches of [3] on a curved grid shell whose bars were aligned in the principle stress directions showed that the von Mises stress could be reduced up to 40% as a result.

In a similar way, [4] produced grid shells in a model scale on the basis of principal stress lines within the framework of additive manufacturing. A slightly different approach is the use of so-called Michell structures. The Michell continuum forms a surface of a bar grid with the smallest volume for the transfer of the load. [5] use this process to generate ribs to stabilize sheets.

A partially interactive approach was followed by [6] who designed an ultra-thin, concrete floor system prototype in which the course of the ribs (in plane and out of plane) was generated using an iterative form-finding process (with Rhino Vault [7, 8]) so that only compressive stresses exist. However, the fact that the ribs are approximated to the principal stress lines is due to an appropriate manual definition of the initial geometry for shape optimization.

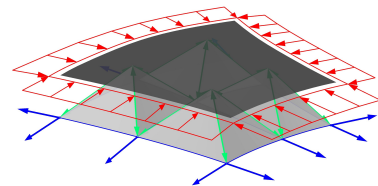
The approach followed in this paper is based on a computation of a quadrangular principal-stress-mesh (PSM). From the PSM the folding structure is derived, whose edges are aligned with the principal stress directions. In the classical calculation of stress lines using the numerical Runge-Kutta method, all parameters (distance and course) are difficult to influence, which is why the lines to be materialized are selected manually in [4, 6]. In contrast to the stress lines, all properties can be parametrically controlled in PSM with the goal of an efficient materialization.

### 3 General Configuration and Load-Bearing Behavior of the Folding Structure

In order to achieve a self-supporting structure without the requirement of a substructure, at least a two-layer structure of the folded structure presented (cf. Figure 1) is necessary.

The load-bearing behavior of such a structure can be compared with the characteristics of a space framework (cf. inset):

Under a positive bending, the compress forces acting over the entire surface in the top layer and the opposite tensile forces in concentrated form in the aligned folded edges on the underside. In contrast to a bar structure, the shear force is not derived from shear forces in the cross section, but dissolved from membrane stresses of the involved partial surfaces, while the characteristic load bearing behavior of folds is also reflected in this case, in that the stresses are concentrated and transferred via the sides of the pyramid.



## 4 Form-Finding of the Stress Adapted Folding Structure

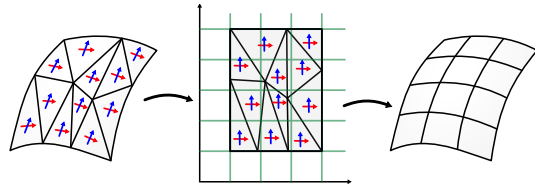
Our form-finding of the stress adapted folding structure can essentially be divided into three core processes (cf. Figure 1): Starting from an initial surface which represents the underside of the planned structure, the principal stresses and principal tension directions are first computed. The principal stresses and are used to calculate a PSM whose edges follow these directions (Section 4.1). The folding structure is then derived from the PSM in a three-stage construction process by punctually folding the tessellated sub-surfaces of the mesh so that the base edges of the pyramidal folds reflect the trajectories. The top part of the two-layer structure forms a flat sheet metal layer.

In many cases, however, geometric alignment alone is not enough to use the material most efficiently, since they only determine the directions of the support axes of a system. If the folding pattern is only aligned according to the main stress direction, it can happen that the material or the stiffness of the structure is not distributed according to the stresses. For this reason, it is also necessary to include the stress *magnitudes* (normal stresses) in the form-finding process in addition to the principal stress *directions* (Section 4.2).

### 4.1 Principal Stress Mesh Generation

The generation of the principal stress direction aligned mesh is based on the *Mixed-Integer Quadrangulation* (MIQ) method of Bommes et al. [9]. The MIQ algorithm generates a quadrilateral mesh from a given triangular input mesh in two main steps: the computation of a smooth cross field based on a sparse set of directional constraints (typically extracted from the curvature of the input mesh) followed by the computation of a parametrization which aligns to that cross field. Since in our case the alignment is given by the principal stress directions which are defined on the whole surface, the computation of the cross field is of less interest for us and we will concentrate on the computation of the parametrization in the following paragraph.

The parametrization consists of a pair of piecewise linear scalar functions  $u$  and  $v$  mapping each triangle of the input into the two-dimensional plane. The quadrangular mesh is then obtained by lifting the regular grid consisting of all lines in the two-dimensional domain for which one of the coordinates is a constant integer back onto the input object.



The two function  $u$  and  $v$  are found by minimizing the following energy for each triangle  $t$ :

$$E_t = \|h\nabla u_t - \mathbf{u}_t\| + \|h\nabla v_t - \mathbf{v}_t\| \quad (1)$$

where  $h$  is the desired edge length of the quadrangular mesh,  $\mathbf{u}_t$  and  $\mathbf{v}_t$  define the desired local alignment of the quads and  $\nabla u$  and  $\nabla v$  are the gradients of the  $u$  and  $v$  function, respectively. In contrast to Bommes et al. who compute  $\mathbf{u}_t$  and  $\mathbf{v}_t$  by interpolating a set salient directions calculated from the curvature information of the input mesh, we directly use the two principal stress directions to define the alignment.

Functions  $u$  and  $v$  minimizing Equation (1) are simply found by solving a linear system. In addition to the alignment, we also require that singularities in the cross field (points/areas without unique principle stress directions, e.g. symmetrical-points of geometries), are represented by vertices, which is achieved by  $u$  and  $v$  being integers in these location. This way we ensure that chains of edges pass through these points allowing good load ablation. To compute a

parametrization close to the minimizer of Equation (1) fulfilling this additional requirement we use the algorithm presented by Lyon et al. [10].

#### 4.2 Mesh Densification

To achieve the most homogeneous and efficient material utilization as possible, in addition to the geometric alignment according to the principal stress *directions*, the inclusion of the associated principal stress *magnitudes* is required.

Although a certain compression of the trajectories can often be observed with increasing stress, this cannot be assumed to be valid in general [11, 12]. Especially in the area of isotropic points – shear force nulls without a clear main stress direction – the opposite can often be observed. In that case, trajectory distances and stresses both increase towards the isotropic point, as the case, for example, of the field center of the square plate in Figure 1. A folding pattern following this mesh leads to a correspondingly higher stress on the structure in the relatively less materialized field center. Thus, it is desirable to increase the mesh density in these regions which we achieve with an iterative algorithm explained in the following paragraph.

For each edge we compute the integral of the stress in direction orthogonal to the edge. If this integral exceeds a certain threshold  $T$  the edge is marked to be split. (To obtain a scale invariant threshold we define  $T$  as a multiple of the minimal computed integral.) The reason behind this is that splitting two opposite edges of a quad is achieved by adding a new edge between the centers of those edges. This in turn leads to an additional crease in the folding structure reducing the load on the two parallel creases.

We add to the already marked edges which exceed the stress threshold a small set of edges such that the number of split edges per quad is even. This leads to a refinement such that the resulting mesh still consists of only quadrilaterals and the new edges form “load paths” which are either closed or connect between boundaries. This process is iterated until no edges remain for which the orthogonal stress integral exceeds the threshold leading to a more homogeneous stress distribution among the creases of our folding structure. Figure 2 shows results of this algorithm for our analyzed systems.

### 5 Results

In this chapter the results of the form optimization will be analyzed from two points of view: In the first part the results of the optimizations are evaluated by comparing the stress adapted folding structures with a corresponding geometrically, regular structure. The second part we examine the question, which load is most effective as the shaping load case when several different loads can act.

#### 5.1 Evaluation of the Optimized Folding Structure

The results of the optimizations are evaluated within the framework of a structural analysis, based on a broad spectrum of different geometries shown in Figure 2.

Due to the differences in structure, area and mass of the structural variants, the evaluation criteria here is efficiency, in which the characteristic load-bearing capacity  $G_c$  is measured in relation to the characteristic self-weight  $R_c$ .

$$E = R_c/G_c \quad (2)$$

Both design variants (stress adapted and regular folding structure) were analyzed in a parametric

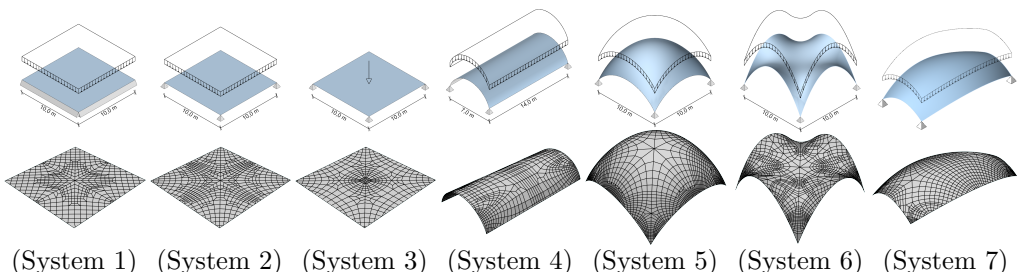


Figure 2: Evaluated geometries (top) and corresponding stress aligned meshes (bottom).

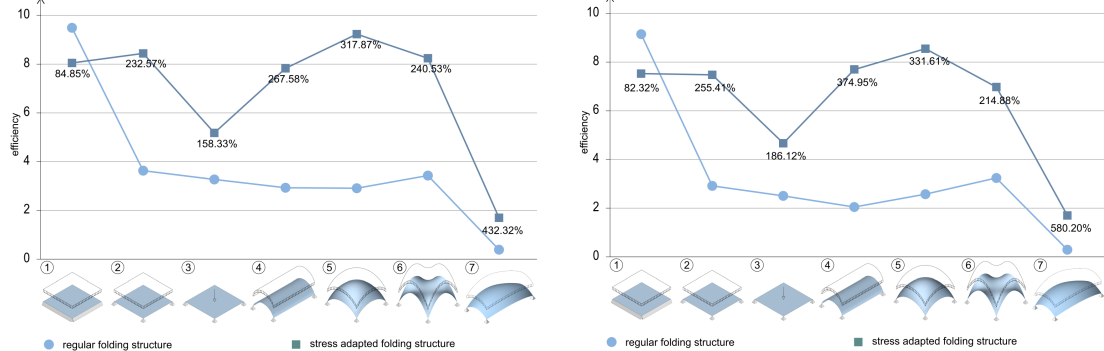


Figure 3: Arithmetic mean values of the three most efficient configurations of the systems in a stress analysis (left) and a buckling analysis (right).

study to determine the most efficient configuration with the associated construction variables height, sheet thickness and folding density. In order to avoid individual evaluations, randomly outstanding maximum values, we consider the average of the three most efficient structures instead. Stress and buckling are evaluated separately and the results are summarized in Figure 3. Comparing only the results, the optimized structures, with the exception of system 1, are much more efficient. They increase in efficiency both in stress analysis and in stability analysis, up to 140% to 580%.

The fact that for system 1 the regular structure is more efficient than the stress aligned one is due to the characteristic load-bearing behaviour of this system. A square, dense grid structure comes closest to square, linearly supported plate with a uniform load, which theoretically has an infinite number of support axes with a circular load transfer (cf. Figure 4 left). Systems with a concentrated load transfer/support axes behave differently, for example system (cf. Figure 4 right). The associated stress diagram illustrates in a clear way how the loads in the stress adapted variant are primarily transmitted to the corner bearings via the correspondingly aligned folds – from the center of the plate via the diagonal support axes and near the plate edges via the support axes running parallel to these.

This phenomenon could basically be observed within the scope of the study: The more concentrated the load of a system is transferred, the more effective and efficient is a folding structure aligned accordingly.

However, this does not mean, that a stress adapted folding structure is necessarily more efficient in every design configuration, but it does lead to a more efficient construction with a corresponding configuration parameters in most cases.

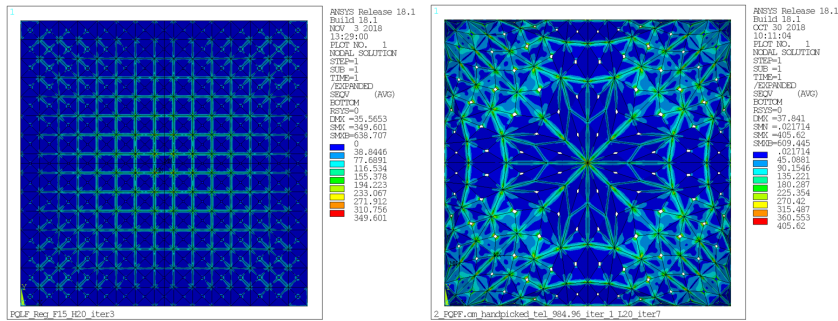


Figure 4: Plot of Mises stress for a regular structure (left) and a stress aligned structure (right).

## 5.2 The Form Shaping Load

After it is been confirmed that an alignment of the folding pattern according to the stresses significantly increases the efficiency of the structure, the following question arises: Which load is to consider in the form finding process as a shaping load case when different loads can act alternatively or simultaneously? Especially when it comes to lightweight construction, the stresses from the dead load are lower than that from the life load and thus not the shaping load case. For this purpose, we analysed a double-curved geometry which for three different load cases were considered (each of the same load sum). The three load cases are (1) the dead load, (2) a point load and (3) a horizontal load (cf. Figure 5). In addition to the individual loads, also the three possible combinations of the dead load with the other two loads (1+2, 1+3, and 1+2+3) were considered. For each load case and combination, we derived the stress adapted folding structure as discussed in Section 4, while the densification (Section 4.2) was not taken into account in order just to evaluate the alignment to the stress directions. All six structures were analyzed with all load cases also within an elastic stress analysis. Therefore, the evaluation here is not based on the load capacity, but on a comparative value that makes a statement about the overall load-bearing behavior. For this reason, the sum of the stresses of all nodes was evaluated, with the same total area of the structures and number of FE-elements.

Figure 7 shows the stress sum for all combinations of load cases and the resulting structures. Comparing all the graphs, it is noticeable that they describe the same general shape for all load cases. When evaluating these graphs, the areas of the individual load cases (1-3) and the combinations are to be considered separately: For the individual load cases, it can be stated for cases 1 and 2 that the associated structures are better solution. In load case 3 (horizontal load) this is not true. For this type of load, the structures of 1 and 2 are more favorable. The stresses of load case 3 lead to relatively “chaotic” suspension shafts, with many tight curvature and

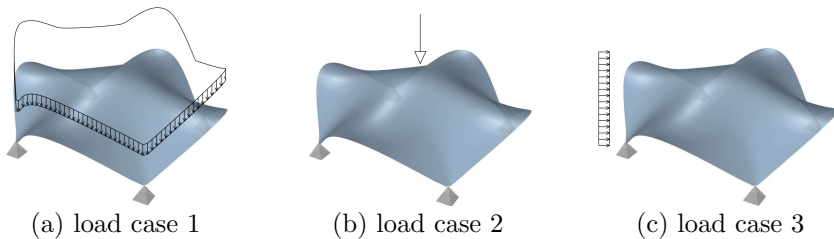


Figure 5: Three different load cases on a doubly curved surface: load case 1: dead load (left), load case 2: point load (center) and load case 3: horizontal load (right).

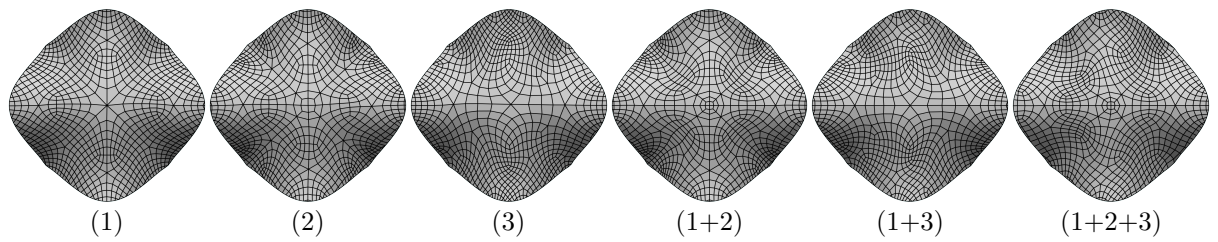


Figure 6: Resulting meshes for the different combinations of load cases shown in Figure 5.

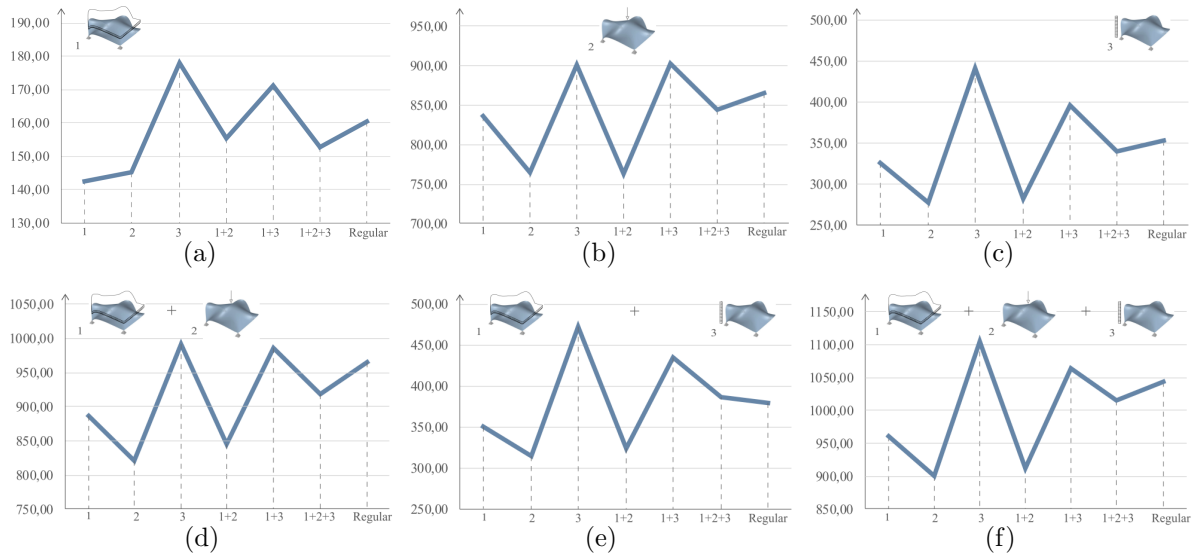


Figure 7: Stress sum [ $\cdot 10^3 \text{ N/mm}^2$ ] of the structure based on the meshes in Figure 6 with the load cases in Figure 5

direction changes, which cannot be implemented in that detail by a coarser folding structure, so that also the homogeneously regular structure turns out better. This also has an effect on combined load cases. Load case 3 effects the meshes (1 + 2, 1 + 3) unfavorably. The second reason is the density of the folds. Whereas in cases 1, 2 and 1+2 the folds “naturally” concentrate on the stress-intensive support areas, this does not apply to load case 3. This confirms the statement, that the more concentrated the load is transferred with well-structured support axes, the more effective and efficient the alignment effects and pure alignment to the stress directions without taking the stress magnitudes into account does not necessarily lead to the most efficient structure.

## 6 Conclusion

This paper shows a shape optimization approach for folding structures based on the calculation of a principal stress mesh. In order to increase the efficiency, the geometrical alignments according to principal stress direction as well as the stress magnitudes were included. The evaluation of the approach was based on different geometries according to their efficiency, i.e. the ratio of the load capacity to the self weight.

The question about the forming load case, when several different loads can occur corroborate the following theses: If the stresses are not included in the form determination, the load case

used as a basis for the form finding does not necessarily lead to the most sustainable or efficient structure for this load case.

However, the comparison showed that the optimized designs with alignment to the principal stress directions and adapted to principal stress magnitudes can improve the efficiency by up to 480% over simple regular structures.

Even once the optimal folding pattern has been generated, the question remains as to the most efficient construction parameters such as material thickness and folding height to fully exploit the potential of the stress-adapted mesh. Further research could be carried out and, e.g. the stiffness values of such a folding pattern could be simulated using analytical or numerical methods.

## 7 Acknowledgements

This work was funded by the Deutsche Forschungsgemeinschaft (DFG, German Research Foundation) - project 269321250.

## References

- [1] R. Herkrath and M. Trautz, “Starre Faltungen als Leichtbauprinzip im Bauwesen,” *Bautechnik*, vol. 88, no. 2, pp. 80–85, 2011.
- [2] Z. H. Architects and Bollinger + Grohmann, “Ciab pavilion beijing 2013.” <https://www.karamba3d.com/projects/ciab-pavilion/>, Last accessed 10 June 2019.
- [3] M. Dimcic, *Structural optimization of grid shells based on genetic algorithms*. Dissertation, University of Stuttgart, 2011.
- [4] K.-M. M. Tam, J. R Coleman, N. W Fine, and C. Mueller, “Stress line additive manufacturing (slam) for 2.5-d shells,” 2015.
- [5] F. Gil-Ureta, N. Pietroni, and D. Zorin, “Structurally optimized shells,” *CoRR*, vol. abs/1904.12240, 2019.
- [6] D. López, D. Veenendaal, M. Akbarzadeh, and P. Block, “Prototype of an ultra-thin, concrete vaulted floor system,” 2014.
- [7] M. Rippmann, L. Lachauer, and P. Block, “Rhinovault - interactive vault design,” *International Journal of Space Structures*, vol. 27, no. 4, pp. 219–230, 2012.
- [8] M. Rippmann and P. Block, “Funicular shell design exploration,” in *Proceedings of the 33rd Annual Conference of the ACADIA*, (Waterloo/Buffalo/Nottingham, Canada), 2013.
- [9] D. Bommes, H. Zimmer, and L. Kobbelt, “Mixed-integer quadrangulation,” *ACM Transactions on Graphics*, vol. 28, no. 3, pp. 77:1–77:10, 2009.
- [10] M. Lyon, M. Campen, D. Bommes, and L. Kobbelt, “Parametrization quantization with free boundaries for trimmed quad meshing,” *ACM Trans. Graph.*, vol. 38, no. 4, 2019.
- [11] D. H. and R. Moufang, *Forschung im Ingenieurwesen*, vol. 12, ch. Kritik des Kraftflußbegriffes. Springer Berlin Heidelberg, 1941.
- [12] U. Wegner, *Über den Zusammenhang zwischen Strömungs- und Spannungsproblemen*, vol. V, ch. Kritik des Kraftflußbegriffes. Springer Verlag, 1934.